Sensitivity and Uncertainty Analysis of IAEA CRP HTGR Benchmark Using McCARD

Sang Hoon Jang and Hyung Jin Shim*
Department of Nuclear Engineering, Seoul National University, 1 Gwanak-ro, Gwanak-gu, Seoul 151-744
alixus@snu.ac.kr, shimhj@snu.ac.kr *

1. Introduction

For the purpose of verification on design features and evaluation on safety performance of developing high temperature gas cooled reactors (HTGRs), the Technical Working Group on Gas Cooled Reactor (TWG-GCR) launched a series of benchmark problems regarding the uncertainty analysis in modeling (UAM) via IAEA Coordinated Research Program (CRP) on HTGR [1]. The benchmark consists of 4 phases starting from the local standalone modeling (Phase I) to the safety calculation of coupled system with transient situation (Phase IV). As a preliminary study of UAM on HTGR, this paper covers the exercise 1 and 2 of Phase I which defines the unit cell and lattice geometry of MHTGR-350 (General Atomics). The objective of these exercises is to quantify the uncertainty of the multiplication factor induced by perturbing nuclear data as well as to analyze the specific features of HTGR such as double heterogeneity and self-shielding treatment.

The uncertainty quantification of IAEA CRP HTGR UAM benchmarks were conducted using first-order AWP method in McCARD. Uncertainty of the multiplication factor was estimated only for the microscopic cross section perturbation. To reduce the computation time and memory shortage, recently implemented uncertainty analysis module in MC wielandt calculation was adjusted [2]. The covariance data of cross section was generated by NJOY/ERRORR module with ENDF/B-VII.1. The numerical result was compared with evaluation result of DeCART/MUSAD code system developed by KAERI.

2. Methodologies

There are two ways of quantifying uncertainty of nuclear parameters in MC approach. One is the direct stochastic sampling method of running MC simulation several times with perturbed nuclear data. Though the computing power today is quite advanced, this approach is quite time-consuming and burdensome. Another approach is the sensitivity and uncertainty (S/U) analysis which utilize the sensitivity of nuclear parameter to acquire the uncertainty through error propagation model. There have been many studies on perturbation methods and their application for benchmark problems. In MCNP5, the conventional perturbation methods such as correlated sampling and the second-order differential operator sampling (DOS) are implemented and compared their accuracy for fixed source problem [3]. These two methods show drawbacks on estimating effect of the fission source perturbation [4]. In MCNP6 and SCALE-6.1, an alternative technique of the adjoint-weighted perturbation (AWP) method is implemented and compared with DOS method for k-eigenvalue problems [5]. As for McCARD, the first-order AWP method based on adjoint flux from MC forward calculation is implemented and shows equivalence of the method with first-order DOS [6].

In MC simulation, the uncertainty of desired value Q can be propagated from various sources including geometric model, material composition, cross section data and etc. If we consider the cross section data to be the only source of uncertainty, the variance of Q is decomposed into two terms as equation (1), using uncertainty propagation formula [7].

$$\sigma^2[Q] = \sigma_S^2[Q] + \sigma_{XX}^2[Q] \tag{1}$$

The two terms in the right hand side represent the statistical error and the error propagated from cross section uncertainty as equation (2) and (3).

$$\sigma_S^2[Q] = \lim_{n\to\infty} \frac{1}{n-1} \sum_{k=1}^{n} (Q_k - \langle Q_k \rangle)^2 \tag{2}$$

$$\sigma_{XX}^2[Q] = \sum_i \sum_\alpha \sum_g \sum_{i'} \sum_{\alpha'} \sum_{g'} \mathrm{cov}[x_{\alpha,g}^i, x_{\alpha',g'}^{i'}] \left(\frac{\partial \langle Q \rangle}{\partial x_{\alpha,g}^i}\right) \left(\frac{\partial \langle Q \rangle}{\partial x_{\alpha',g'}^{i'}}\right) \tag{3}$$

In equation (3), x, i, α, g and < > denote microscopic cross section, nuclide, reaction type, energy group and expectation operator, respectively. With the approximation of the derivative terms with equation (4) and the definition of correlation coefficient, the equation (3) is rearranged to equation (5).

$$\frac{\partial \langle Q \rangle}{\partial x_{\alpha,g}^i} \cong \frac{\langle Q(\overline{x_{\alpha,g}^i} + \sigma(x_{\alpha,g}^i)) \rangle - \langle Q(\overline{x_{\alpha,g}^i}) \rangle}{\sigma(x_{\alpha,g}^i)} = \frac{\delta \langle Q(\overline{x_{\alpha,g}^i}) \rangle}{\sigma(x_{\alpha,g}^i)} \tag{4}$$

$$\sigma_{XX}^2[Q] = \sum_i \sum_\alpha \sum_g \sum_{i'} \sum_{\alpha'} \sum_{g'} \rho[x_{\alpha,g}^i, x_{\alpha',g'}^{i'}] \delta\langle Q(\overline{x_{\alpha,g}^i}) \rangle \delta\langle Q(\overline{x_{\alpha',g'}^{i'}}) \rangle \tag{5}$$

To calculate the error induced by the cross section uncertainty, correlation coefficient and the variation of

expected value Q are needed. The former one can be made by processing cross section data with NJOY/ERRORR module, and the later one can be calculated by the MC perturbation method or direct subtraction method.

3. MHTGR-350 Modeling

3.1 Exercise I-1

Exercise I-1 stands for local neutronic cell physics with single fuel compact of MHTGR-350. The unit cell consists of cylindrical UCO fuel compact, helium gap and surrounding prismatic block graphite. In Ex.I-1a, fuel region is homogenized with TRISO fuel particle and graphite matrix, whereas explicit model for randomly distributed TRISO fuel particle is specified in Ex.I-1b. Fig 1 shows unit cell of homogenized model and explicit model. TRISO particle is composed of 5 layers, which are UCO (15.5 w/o) fuel kernel, porous carbon buffer, inner pyrolytic carbon, silicon carbide, and outer pyrolytic carbon. The packing fraction of TRISO particle in the compact is 0.35.

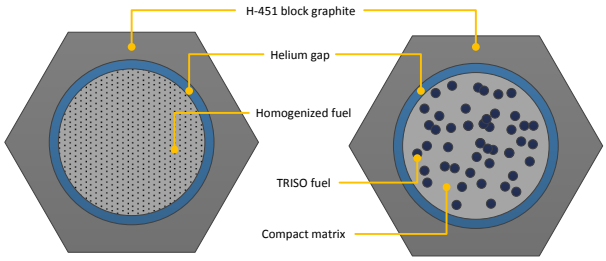

Fig. 1. Unit cell models of Ex.I-1a (left) and Ex.I-2a (right)

3.2 Exercise I-2

Exercise I-2 stands for local neutronic lattice physics with fuel assembly of MHTGR-350. Ex.I-2a and I-2b have single fuel assembly of fresh fuel and depleted fuel respectively, while Ex.I-2c has a simplified super cell model which combines fresh fuel, depleted fuel and reflector assemblies.

Fig 2 shows the fuel assembly model. The fuel assembly consists of 210 fuel compacts, 102 large coolant channels, 6 small coolant channels and 7 block graphite around center position, and 6 lumped burnable poison (LBP) compacts at the 6 corners. LBP compact has similar structure with fuel compact. It is composed of cylindrical compact region with randomly distributed B_4C particles, helium gap and block graphite. The particle has 3 layers of B_4C kernel, porous carbon buffer, and pyrolytic carbon. The packing fraction of LBP particle is 0.109.

As for Ex.I-2b, the depleted fuel assembly shares the same model with Ex.I-2a except for the fuel composition and LBP compact. The fuel composition of depleted fuel is given by the benchmark specification obtained from Serpent depletion calculation without LBP up to 100MWd/kgU. The region inside of the LBP compact surrounded by helium gap is substituted with the H-451 block graphite.

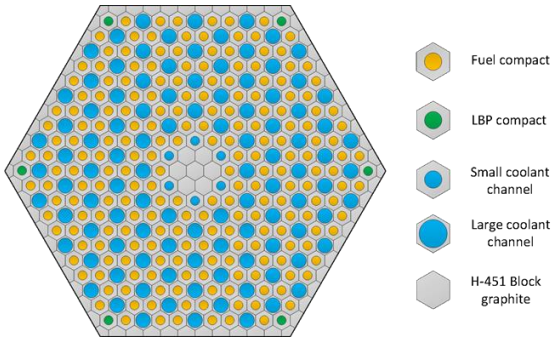

Fig. 2. Fuel assembly model of Ex.I-2

Fig 3 presents the super cell model. Super cell model is composed of one fresh fuel assembly surrounded by depleted fuel assemblies on one side and reflectors on other sides. The fresh fuel assembly has explicit heterogeneous model, while depleted fuel assembly and reflector have simplified homogenous models. For the composition of depleted fuel region, the number of nuclides is reduced for simplification compared with Ex.I-2b.

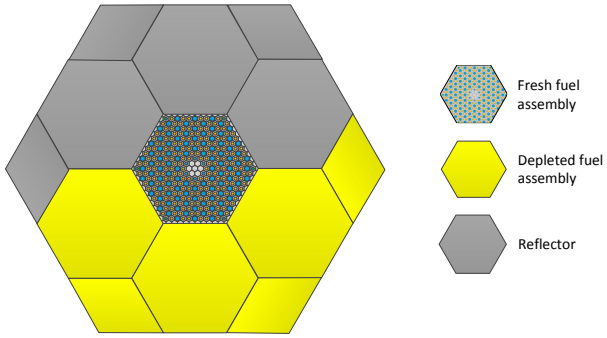

Fig. 3. Super cell model of Ex.I-2c

4. Numerical Result

4.1 Calculation Options

For Ex.I-1, calculations were done with both CZP and HFP conditions, while calculations for Ex.I-2 were done under only HFP condition. The temperatures of material are given in Table I for each condition.

Table I: Temperature of CZP and HFP condition

	CZP	HFP
Fuel compact [K]	600	1200
Helium gap [K]	600	1000
H-451 block graphite [K]	400	1000
Coolant channel [K]	-	1000

Eigenvalue calculations were done with two cross section libraries of ENDF/B-VII.0 and ENDF/B-VII.1. The covariance data for MC perturbation calculation was processed using NJOY/ERRORR module with HELIOS 190 energy group structure from ENDF/B-VII.1 library. Every calculation was done with 100,000 histories per cycle and the number of inactive cycle and active cycle were set to 50 and 200 respectively. DBRC option was used for ^{238}U.

4.2 Eigenvalue Calculation

The numerical results of McCARD eigenvalue calculation with ENDF/B-VII.0 and ENDF/B-VII.1 library are summarized in table II and III respectively. In both tables, McCARD results are compared with the Serpent results. The effect of double heterogeneity shows significant reduction of resonance self-shielding in the volume weighted homogenized cases (Ex.I-1a) than the explicitly modeled cases (Ex.I-1b). The Doppler broadening effect which is mainly attributed to resonance of ^{238}U shows negative feedback on multiplication factor.

Table II: McCARD eigenvalue calculation results with ENDF/B-VII.0

	EDNF/B-VII.0	
	Serpent	McCARD
	k_{inf} (SD)	k_{inf} (SD)
Ex.I-1a CZP	1.25995 (0.00012)	1.26051 (0.00012)
Ex.I-1a HFP	1.18462 (0.00014)	1.18430 (0.00013)
Ex.I-1b CZP	1.31865 (0.00012)	1.32038 (0.00017)
Ex.I-1b HFP	1.24657 (0.00013)	1.24767 (0.00018)
Ex.I-2a HFP	1.06304 (0.00008)	1.06133 (0.00018)
Ex.I-2b HFP	0.96528 (0.00013)	0.96592 (0.00015)
Ex.I-2c HFP	1.05010 (0.00005)	1.04943 (0.00017)

Table III: McCARD eigenvalue calculation results with ENDF/B-VII.1

	EDNF/B-VII.1		EDNF/B-VII.1*
	Serpent	McCARD	McCARD
	k_{inf} (SD)	k_{inf} (SD)	k_{inf} (SD)
Ex.I-1a CZP	1.25841 (0.00013)	1.25910 (0.00011)	1.25954 (0.00018)
Ex.I-1a HFP	1.18357 (0.00015)	1.18313 (0.00017)	1.18330 (0.00017)
Ex.I-1b CZP	1.31767 (0.00012)	1.31911 (0.00017)	1.31905 (0.00017)
Ex.I-1b HFP	1.24525 (0.00014)	1.24628 (0.00017)	1.24658 (0.00017)
Ex.I-2a HFP	1.06177 (0.00008)	1.05610 (0.00020)	1.06017 (0.00020)
Ex.I-2b HFP	0.96619 (0.00013)	0.96691 (0.00016)	0.96694 (0.00016)
Ex.I-2c HFP	1.04341 (0.00004)	1.05263 (0.00018)	1.04281 (0.00017)

*ENDF/B-VII.0 is used for thermal scattering data of graphite.

For the case of Ex.I-2a and Ex.I-2c, significant discrepancies are found in ENDF/B-VII.1 cases. This was found to be the effect of the thermal scattering data of graphite. The fourth column is the result after substituting graphite data from ENDF/B-VII.1 to ENDF/B-VII.0 and it shows good consistency with other results.

4.3 Sensitivity and Uncertainty Analysis

S/U analysis was done with the Ex.I-1 cases. Table IV compares the uncertainty of multiplication factor induced by the perturbed cross section of ^{235}U and ^{238}U. The McCARD results match well with the DeCART/MUSAD results except for the case induced from the covariance data between ^{238}U capture reactions. In the ^{238}U capture cases, McCARD underestimates the uncertainty by 30% and this difference is induced by implicit uncertainty which is related to resonance self-shielding effect. The research on resonance self-shielding effect in uncertainty quantification of G. Chiba [8] shows similar overestimation of uncertainty in the case of inconsistent methodology which do not consider the resonance self-shielding effect.

Table IV: Comparison result of McCARD S/U analysis with DeCART/MUSAD

	Uncertainty (% $\Delta k/k$)			
Reaction Type of covariance data	Ex.I-1a HFP		Ex.I-1b HFP	
	McCARD	DeCART/ MUSAD	McCARD	DeCART/ MUSAD
$^{235}U\ \nu-\nu$	0.610	0.610	0.612	0.613
$^{235}U\ cap-cap$	0.236	0.236	0.238	0.237
$^{235}U\ cap-fis$	0.074	0.074	0.074	0.073
$^{235}U\ fis-fis$	0.073	0.073	0.071	0.071
$^{238}U\ \nu-\nu$	0.008	0.009	0.009	0.008
$^{238}U\ cap-cap$	0.445	0.602	0.388	0.574
$^{238}U\ cap-fis$	0.002	0.002	0.002	0.002
$^{238}U\ fis-fis$	0.002	0.002	0.002	0.001
total	0.801	0.896	0.773	0.878

5. Conclusion

IAEA CRP HTGR UAM benchmark problems were analyzed using McCARD. The numerical results were compared with Serpent for eigenvalue calculation and DeCART/MUSAD for S/U analysis. In eigenvalue calculation, inconsistencies were found in the result with ENDF/B-VII.1 cross section library and it was found to be the effect of thermal scattering data of graphite. As to S/U analysis, McCARD results matched well with DeCART/MUSAD, but showed some discrepancy in ^{238}U capture regarding implicit uncertainty.

For the future work, research on the effect of thermal scattering library of graphite on HTGR will be conducted through S/U analysis for the differences between the cross section data from ENDF/B-VII.0 and ENDF/B-VII.1. Also, the S/U analysis for the remaining part of the benchmark including Ex.I-2 will be continued.

REFERENCES

[1] "IAEA Coordinated Research Project on HTGR Reactor Physics, Theral-hydraulics and Depletion Uncertainty Analysis," draft rev 4. , *IAEA*, (2014)

[2] S. H. Choi and H. J. Shim, Adjoint Sensitivity and Uncertainty Analysis in Monte Carlo Wielandt Calculations," *ANS MC2015, Joint International Conference on Mathematics and Computation (M&C), Supercomputing in Nuclear Applications (SNA) and the Monte Carlo (MC) Method*, Nashville, TN, Apr, 19-23, 2015, on CD-ROM, American Nuclear Society, LaGrange Park, IL (2015)

[3] H. Tao, and Su Bingjing, "Comparison between Correlated Sampling and the Perturbation Technique of MCNP5 for Fixed-Source Problem," *Annals of Nuclear Energy*, **38**[6], pp. 1318-1326 (2011).

[4] Y. Nagaya and T. Mori, "Impact of Perturbed Fission Source on the Effective Multiplication Factor in Monte Carlo Perturbation Calculations," *J. Nucl. Sci. Technol.*, **42**[5], 428 (2005).

[5] C. Brian and B. Forrest, "Comparison of the Monte Carlo Adjoint-Weighted and Differential Operator Perturbation Methods," *P. Nucl. Sci. Technol.*, **2**, pp 836-841 (2011).

[6] H. J. Shim and C. H. Kim, "Adjoint Sensitivity and Uncertainty Analyses in Monte Carlo Forward Calculations," *J. Nucl. Sci. Technol.*, **48**[12], pp 1453-1461 (2011).

[7] H. J. Park, H. G. Joo, H. J. Shim, C. H. Kim and C. S. Gil, "Effect of Cross Section Uncertainties on Criticality Benchmark Problem Analysis by McCARD," *Journal of Korean Physical Society*, Vol. 59, No. 2, pp 1252-1255 (2011).

[8] G. Chiba, A. Tsuji and T. Narabayashi, "Resonance Self-shielding Effect in Uncertainty Quantification of Fission Reactor Neutronics Parameters," *Nucl. Eng. Technol.*, 46[3], 281 (2014).